Morphological, Thermal and Electrical Properties of (PEO/PVP)/ Au Nanocomposite Before and After Gamma-Irradiation

E.M. Abdelrazek[1,2], A.M. Abdelghany[3], S.I. Badr[2] and M.A. Morsi[4,*]

[1]*Physics Department, Faculty of Science, Taibah University, Al-Ula, Saudi Arabia*

[2]*Physics Department, Faculty of Science, Mansoura University, Mansoura, 35516, Egypt*

[3]*Spectroscopy Department, Physics Division, National Research Center, Cairo, 12311, Egypt*

[4]*Engineering Basic Science Department, Faculty of Engineering, Egyptian Russian University, Cairo, 11829, Egypt*

Abstract: Gold nanoparticles (Au NPs) have been successfully biosynthesized by *Chenopodium murale* (*C. murale*) leaf extract. Au NPs were incorporated within polyethylene oxide (PEO)/polyvinyl pyrrolidone (PVP) polymer blend by casting method. Scanning electron microscope (SEM), Differential scanning calorimetry (DSC), and DC electrical resistivity were used to investigate the morphological, thermal, and electrical properties of blend/Au nanocomposite before and after gamma-irradiation at different doses (1, 2, 3, 4 and 5 MR).SEM micrographs confirmed the dispersion of Au NPs within the polymeric matrix due to effect of irradiation process. DSC analysis showed that the thermal stability for irradiated samples was improved as compared with pure blend and its nanocomposite. DC measurements revealed nonlinear behavior for electrical resistivity versus temperature. The electrical resistivity values for blend/Au nanocopmosite and its high irradiated samples were less compared to pure blend.

Keywords: Gamma-irradiation, Au NPs, SEM, DSC, electrical resistivity.

1. INTRODUCTION

Polymer blending is an essential way to obtain new polymeric materials for newer potential materials with a wide variety of applications. The main advantages of polymer blends are that the properties of the final product can be tailored to the requirements of the applications, which cannot be obtained alone by one polymer [1, 2]. PEO is a semi-crystalline polymer which has both crystalline and amorphous phases at room temperature due to high regularity of its structural unit. PEO is a linear polymer with enteric linkages (i.e. ether group C-O-C) and can solvate different types of inorganic salts. But, a high ordering of PEO structure restricts its conductivity so it must be coupled with amorphous polymer [3, 4]. PVP deserve a special attention among the conjugated polymers due to its easy process ability, good environmental stability, moderate electrical conductivity and rich physics in charge transport mechanism. Also, it is an amorphous polymer and possesses high T_g due to the existence of the rigid pyrrolidone group, which is strong on drawing the group and is known to make various complexes with other polymers. Thus, it can allow faster ionic mobility compared with other semi-crystalline polymers having low scattering losses for different applications [1, 2].

In recent days, polymer nanocomposites are being considered as versatile materials in many scientific applications leading to technological advancements. This is because of the fact that embedding of the nanoparticles into polymer matrix significantly effects on its thermal, optical and electrical properties while retaining its inherent characteristics [5, 6]. Thus, polymer nanocomposites open a new gateway in developing the materials for improved performance in many potential applications like, optical devices, biomedical science, coating materials and electrochemical applications [7-9]. Gold nanoparticles (Au NPs) have been widely studied in the past 10 years due to their unique properties, such as quantum size effect, catalysis, and optical and electrical properties [10-12]. Hsu *et al*. [13] found an enhancement for the thermal and mechanical properties of polyurethane/Au nanocomposites with low content of Au NPs and the opposite was occurred at higher Au NPs content. Vodnik *et al*. [14] found that the structural and optical properties for (PVA)/ Au nanocomposites were improved but its thermal stability was reduced compared to pure PVA.

The properties of such nanocomposites can further be modified through different treatments like, UV-irradiation, neutron-irradiation and annealing. γ-irradiation is one of the extensively used tools to alter the physical properties of the polymer-metal nanocomposites making these as promising materials for various applications. These modifications are

*Address correspondence to this author at the Engineering Basic Science Department, Faculty of Engineering, Egyptian Russian University, Cairo, 11829, Egypt; Tel: +2 01099258097; Fax: +2 02 28609117; E-mail: m.a_morsi@yahoo.com

because the chemical bond scissions and/or cross-linking induced by high-energetic radiation [15]. When an ionization radiation passes through a polymeric material, excitation and ionization for of the material molecules are existed. These lead to breaking of original bonds, chain scission, radical formation and cross-linking in polymeric material. Eisa *et al*. [16] revealed that gamma irradiation can be used as a size controlling agent for the preparation of Ag NPs filled within PVA. The concentration of Ag NPs was increased with increasing irradiation dose and its average size was largely decreased from 30 nm for PVA/ Ag nanocomposite to 17 nm for PVA/ Ag nanocomposite/75 KGy. Also, Chahal *et al*. [5] found an enhancement for the structural properties and optical parameters, such as optical energy gap and refractive index, of PVA after embedding Ag NPs and exposure to different irradiation doses of γ-rays.

In a previous work [17], we studied the average size for Au NPs and its distribution, structural and optical properties of (PEO/PVP) /Au nanocomposite before and after irradiation process. The main aim of this study has been fundamentally concentrated on the analyzing of the morphological, thermal and electrical properties of (PEO/PVP) blend/Au nanocomposite at different irradiation doses of γ-rays after embedding biosynthesized Au NPs by *Chenopodium murale* extract (*C. murale*) instead of using common hazardous chemicals.

2. EXPERIMENTAL

2.1. Materials

The leaf of *C. murale* was collected from Mansouracity, Dakahlia governorate, Egypt during December 2014. Tetrachloroauric (III) acid trihydrate ($HAuCl_4.3H_2O$, 99.5% GR for analysis) was obtained from Merk, Germany. All the chemicals and solvent used in this study were of analytical grade. Both PEO supplied from ACROS, New Jersey, USA with $M_W \approx$ 40,000gm/mol and PVP from SICO Research Laboratories Pvt. Ltd, Mumbai, India with $M_W \approx$ 72,000gm/mol were used as a basic polymeric materials. The used solvent was double distilled water.

2.2. Biosynthesis of Au NPs and Preparation of PEO/PVP/Au Nanocomposite Films

Preparation of *C. murale* extract and biosynthesis of Au NPs were explained in details in our paper [18]. Fresh leaf extract, used for the biosynthesis of Au NPs, was prepared from 20 g of thoroughly washed leaf in a

500 ml Erlenmeyer flask, boiled in 50 ml distilled water for 1hr and the produced extract was subjected to freeze drying. Suspensions were filtered with Whatman No. 40 filter paper. 100 ml of 5mM aqueous solution of gold chloride was prepared in a Stoppard Erlenmeyer flask. 2 ml of leaf extract (0.2 g/ml) was added at room temperature and the solution pH value was adjusted to 10 with an aqueous solution of 0.1 M HCl and 0.1 NaOH. Pinkish-red color indicated that the formation of Au NPs was observed after 24 hours in dark. Transmission electron microscopy (TEM) micrograph for biosynthesized Au NPs was shown in Figure **1** with average size 2-22 nm.

Polymer blend films were prepared by solution cast technique. A quantity of PEO and PVP (70/30) by weight was dissolved in double distilled water separately and then the polymer blend solution was stirred continuously at room temperature until a homogenous viscous liquid was formed. Further, 0.72 wt. % of Au NPs was added to the PEO/PVP polymer solution under continuous stirring for 24 h. Finally, viscous solutions were poured into polypropylene dishes and the common solvent was allowed to evaporate slowly at room temperature for 2 days to obtain free-standing polymer films at the bottom of dishes. The obtained films were stored in highly evacuated desiccators to avoid any moisture absorption. Film thickness in the range of 0.07–0.09 mm was obtained.
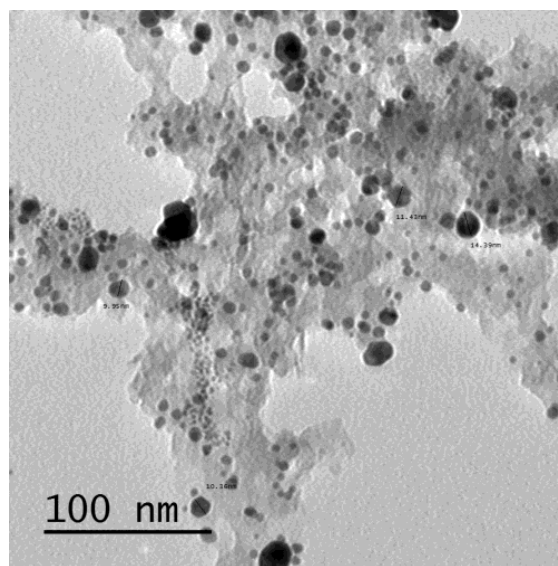
Figure 1: TEM micrographs of the developed Au NPs.

2.3. γ-Irradiation Process

Gamma 1 (type J-3600, Canada, Ltd.) for atomic energy, located at the National Center for Radiation

Research and Technology (Cairo, Egypt), was used. A ^{60}Co source, with an activity of 137,000 Ci, was used for the γ-irradiation of the PEO/PVP/Au nanocomposite films. The irradiation doses (1, 2, 3, 4 and 5 MR) were measured with radiochlormic dye film on Perspex. The dose rate was 2.76kGy/h. The overall error in the dose measurements did not exceed ±4%.

2.4. Measurements

Scanning electron micrograph of the studied samples was performed using SEM Model (JEOLJSM 6510 LV 250, USA), operating at 20KV accelerating voltage. Surface of the samples were coated with 3.5 nm layer of gold to minimize sample charging effects due to the electron beam. DSC curves for the studied samples were recorded using an equipment type (NETZSCH, STA 409CD, Germany) in temperature range from room temperature to 700°C and the heating rate was 10 °C/min in the existence of nitrogen as inert atmosphere. The electrical resistivity was measured using an auto-ranging millimeter (METRISO 5000A, USA) of accuracy ± 0.5 % which applies a standard voltage on the sample and measures the current flowing through it, and gives directly the resistance value. From the sample dimensions and contact geometry, the value of electrical resistivity ρ was calculated. The resistivity of the samples was measured in the temperature range 303–363K.

3. RESULTS AND DISCUSSION

3.1. Scanning Electron Microscopy SEM

Figure **1** shows the SEM micrograph of the surface of pure and filled polymer film without and with gamma irradiation at different doses (1, 2, 3, 4 and 5 MR) at magnification 1,500 times. From Figure **2a**, the image of pure blend PEO/PVP (70/30 wt. %) shows a rough morphology structure which has several crystalline domains i.e. spherulites, due to the semi crystalline nature of blend. After the addition of Au NPs to the pure blend, the size of spherulites is largely decreased and there is an improvement of surface morphology from rough, where the surface texture becomes somewhat smoothened as shown in Figure **2b** for blend/Au nanocomposite. A smooth appearance is generally associated with lowering of PEO/PVP crystallinity. Also, the surface is fully filled with pores where its distribution becomes denser associated with an aggregation for Au NPs on the surface. The existence of pores between Au NPs and polymer blend interfaces is because of the spherulites shrinkage and

is considered as a type of complexation/miscibility between PEO/PVP and Au NPs. Moreover, these pores are corresponding to the interconnected networks of polymers. The enhancement in porosity has been attributed to the enhancement of free ion formation and hence to the enhancement of ionic conductivity. For blend/Au nanocomposite/1-2 MR, number of pores is largely decreased associated with an aggregation for Au NPs, as shown in Figure **2c-d**, due to the existence of structural rearrangement by an irradiation process which gives an opportunity for Au NPs to aggregate. For blend/Au nanocomposite/3 MR, the pores are nearly disappeared as shown in Figure **2e**. This helps the spherulite to exist and thus enhances the degree of crystallinity. With continuous irradiation, the surface texture is changed where the pores are existed again associated with a white halo around it and wrinkle features are occurred on the surface as shown in Figure **2f-g**. Both the distribution and size of pores are increased with increasing the irradiation dose from 4 to 5 MR. This reflects that there is a cross-linked structure within the polymeric matrix and considered the main reason for decreasing the degree of crystallinity [19]. The disappearance of Au NPs aggregation for blend/Au nanocomposite/4-5 MR samples implies that high irradiation process initiates more reduction/growth for Au NPs on the polymer backbone and helps Au NPs to disperse within the polymeric matrix as a result from cross-linked/chain scission within blend/Au nanocomposite/4-5 MR. These observations were in agreement with the results of both X-ray diffraction analysis, ultraviolet/ visible spectroscopy and transmission electron microscope in [17] .

3.2. Differential Scanning Calorimetry (DSC)

DSC is one of the most appropriate ways to show the miscibility and thermal properties of the polymer blends. The glass transition temperature T_g measurement from the DSC thermograms for the polymer blends is utilized to determine its miscibility. An important factor in the new materials development based on polymeric blends is miscibility between the polymers in the blend, because the miscibility degree is directly related to final properties of blend. A miscible polymer blend haves a homogeneous amorphous phase and hence will display a single T_g between the glass transition temperatures of the two polymers.

The DSC curves for pure PVP, pure PEO and PEO/PVP blend (70/30 wt.%) are shown in Figure **3**. DSC curve for PVP shows a broad endothermic
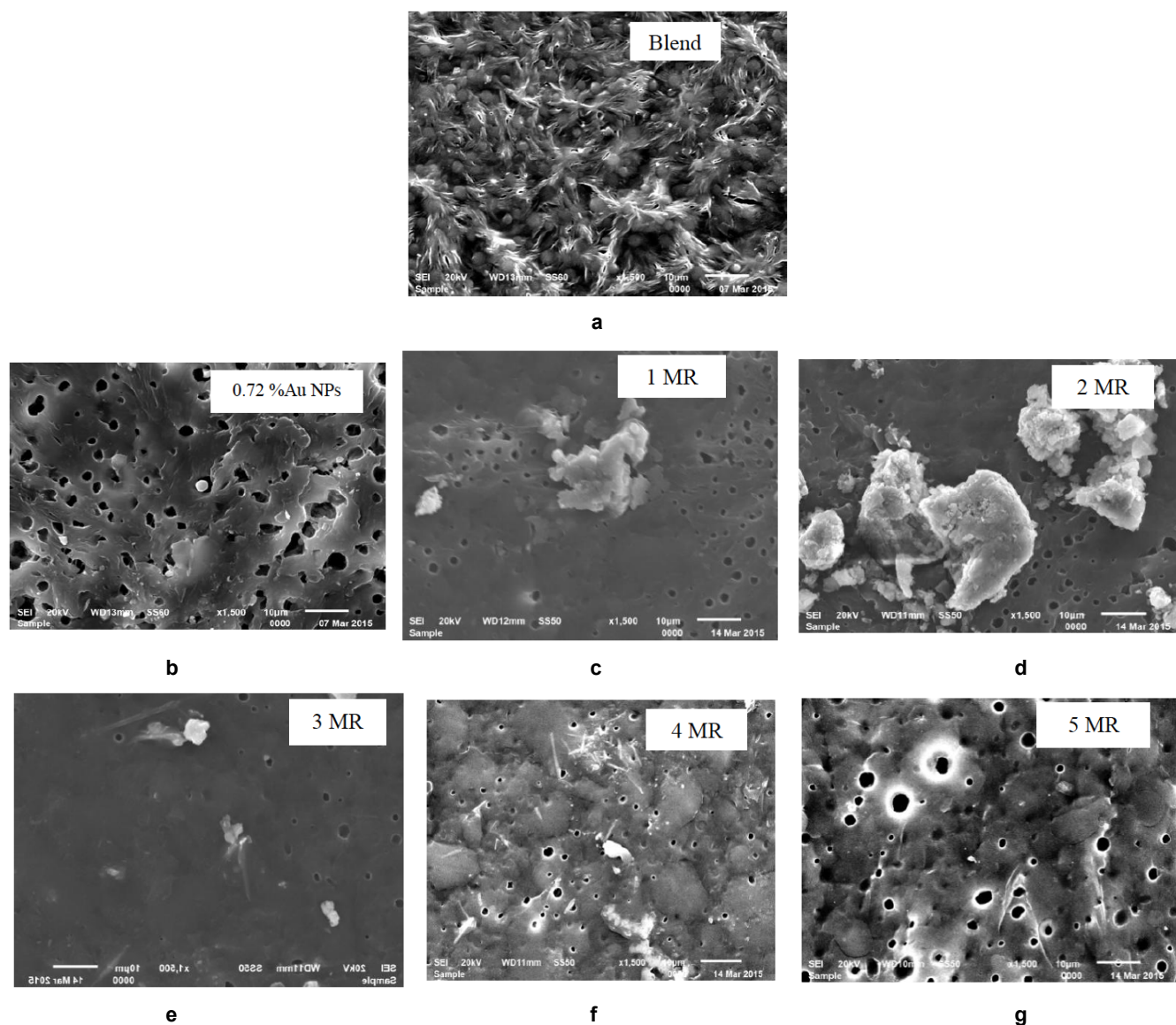
Figure 2: SEM images for pure blend and its nanocomposite before and after γ- irradiation at different doses (1, 2, 3, 4 and 5 MR).

transition at 89.61°C is attributed to T_g. The small endothermic peak centered at about 192.36 °C is attributed to melting temperature (T_m). T_m is very small due to the amorphous nature of PVP as confirmed in XRD analysis. The peaks at about 444.05 and 560.28 °C are referred to the decomposition temperatures T_d [1, 20-22]. From the DSC curve for pure PEO, T_g occurs at -64.68 °C. The melting temperature of the crystalline region of PEO is centered at 68.81 °C. The two endothermic peaks observed at about 339.75 and 416.61 °C are assigned to the decomposition temperatures (T_d) of PEO where the PEO chain undergoes a series of thermal degradation reactions that are able to modify its original structure [23-28]. For pure blend, DSC curve shows a T_g around at 62.13 °C which is often indicated as DSC T_g (onset)-value

relaxation process resulting from micro-Brawnian motion of the main chain backbone where it lies between T_g of the individual components of blend. This implies that the present polymer blend is miscible [27]. The polymer blend exhibited a relatively sharp crystalline melting endotherm (dip) at around 68.82 °C. The melting temperature (T_m) is taken at the apex of the melting endotherm where the polymer becomes completely melted. The decomposition temperatures of blend of blend lies at 344.04 and 426.65 °C.

The DSC curves for pure blend and its nanocomposite before and after γ-irradiation are shown in Figure **4**. All DSC thermograms of the studied samples in the Figure ure exhibited endothermic peaks. The T_g, T_m and T_d values for all investigated films are
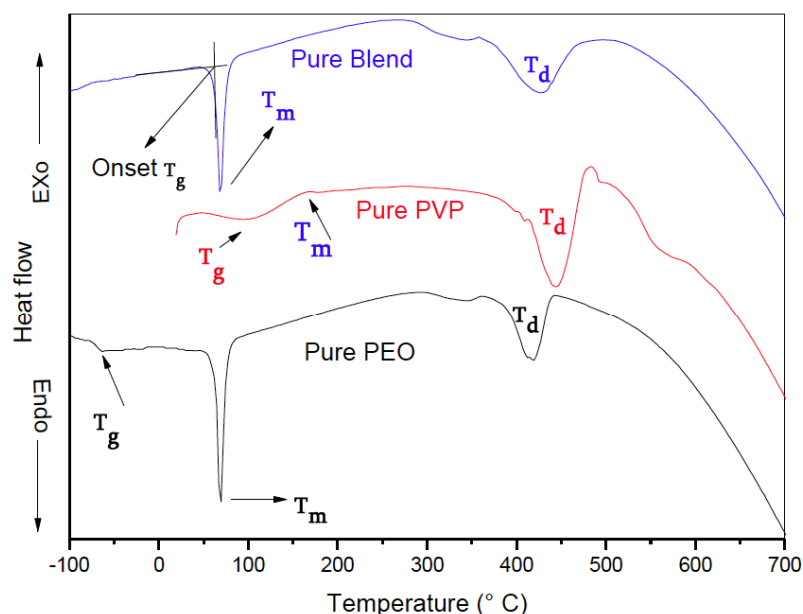
Figure 3: DSC curves for pure PEO, pure PVP and pure PEO/PVP blend.
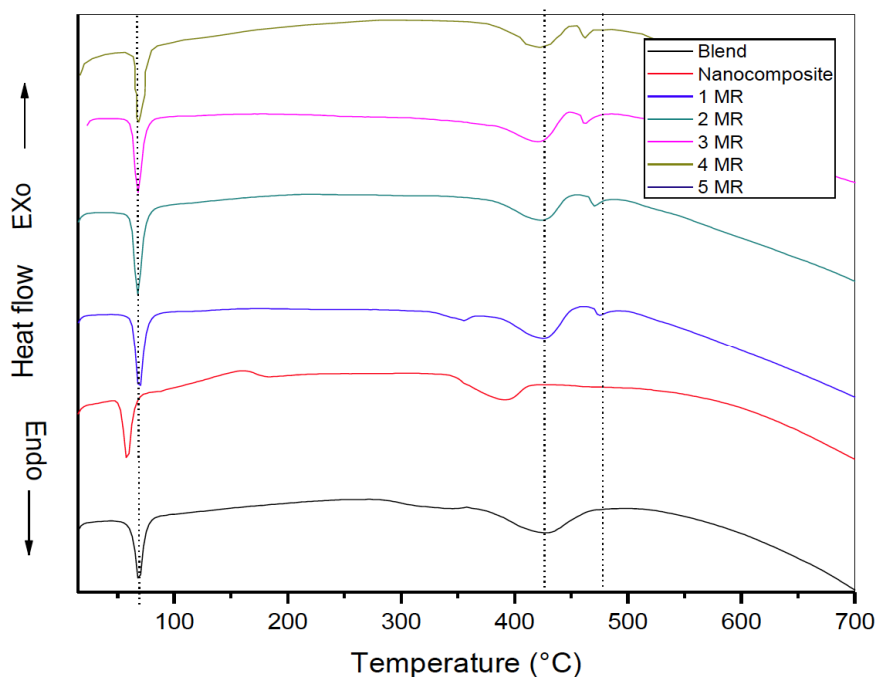
Figure 4: DSC curves for pure blend and its nanocomposite before and after γ- irradiation at different doses (1, 2, 3, 4 and 5 MR).

listed in Table **1**. From this table, it is clear that, the T_g, T_m and T_d valuesare decreased after filling the polymeric matrix of blend. For nanocomposite, the decrease in T_g means that the segmental mobility of amorphous polymer increases due to the addition of Au NPs and become less rigid segments. This means that the Au NPs filler behaves as plasticizer. The decrease of T_m upon Au NPs addition is related to the decrease in the size of spherulites [27, 29] whereas the

crystallites are suppressed. Thus, this leads to an improvement for the amorphous content within the polymer matrix. The DSC curve for blend/Au nanocomposite shows a new exothermic peak at 160.91 °C that can be assigned to the existence of new crystalline phase within the polymeric matrix as a result from Au NPs filling. The position of T_d shifts toward lower temperatures from 426.65 °C to 391.73 °C, implying the formation of intermolecular interactions

between the blend and Au NPs. The existence of such interaction was confirmed by results of SE Mmicrographs.

After irradiation process, the values of T_g and T_m for blend/Au nanocomposite/1-5 MR increases as compared to its values without irradiation. This indicates the γ-irradiation involves structural rearrangements in chains of blend on embedding of Au NPs. Also, the exothermic peak at 160.91 °C is completely disappeared after irradiation as a result from the increase of disorder content within the polymeric matrix. The T_d values for blend/Au nanocomposite/1-5 MR are higher than from blend/Au nanocomposite. This indicates that the γ-irradiation improves the thermal stability for irradiated samples. But, these values are slightly shifted toward lower temperature from 425.02 to 420.27 °C. This result can be attributed to the fine dispersion of Au NPs which increases the disorder content within the polymeric matrix.

More importantly, there is a significant change in the shape of the decomposition peak in DSC curves for irradiated samples; where there is a new endothermic decomposition temperature accompanies the main peak of blend/Au nanocomposite/1-5 MR recorded at 474.78 °C. The split of the decomposition peak in the DSC curve for irradiated samples indicates that the degradation mechanism differs from the nanocomposite before irradiation. The side peak at higher temperature can be attributed to the overlap of the continual eliminations and chain-scission reactions due to irradiation effect which need more energy and occur at a higher temperature [30], where the chain of blend undergoes a series of thermal degradation

reactions that are able to modify its original structure. As a consequence, the blend retains its structure. In other words, DSC curve shows a small endothermic decomposition peak rather than the fundamental one. This endothermic peak may be due to the solid–solid phase transitions followed by the main decomposition peak [31]. Here, such a peak may play a role in the low thermal stability with respect to other studied composites where it shifts toward lower temperature with increasing the irradiation dose. The percentage of relative crystallinity (%χ$_c$) of complexed polymer blend was estimated from the DSC curves using the following equation, assuming that pureblendis 100% crystalline [27].

$$\%\chi_c = \frac{\Delta H_m}{\Delta H_m^0} \times 100 \qquad (1)$$

Where ΔH_m^0 is the crystalline melting enthalpy of pure blend PEO/PVP (found to be 216J/g in the present work) and ΔH_m is the melting enthalpy of blend/Au nanocomposite before and after irradiation that determined from the crystalline melting peaks of studied films. The obtained values of $\%\chi_c$ are summarized in Table **1**. The decrease in $\%\chi_c$ is an indicator for an increase in degree of amorphousity after filling with Au NPs and exposing to high-irradiation doses. Also, the improvement of $\%\chi_c$ values for low-irradiation doses is a measure for an improvement of degree of crystallinity. These observations were in agreement with the results of XRD analysis in [17].

3. 3. DC Resistivity Measurements

Figure **5** shows the variation in electrical resistivity for polymer blend, blend/Au nanocomposite and

Table 1:   Glass Transition (T_g), Melting (T_m), First and Second Decomposition (T_{d1}, T_{d2}) Temperatures and Relative Percentage of Crystallinity ($\%\chi_c$) for Pure Blend, Blend/ Au Nanocomposite and Blend/Au Nanocomposite/1-5 MR

Samples	T_g (onset) (˚C)	T_m (˚C)	T_{d1} (˚C)	T_{d2} (˚C)	T_d^* (˚C)	$\%\chi_c$	E_a(eV)
Pure blend PEO/PVP	62.13	68.82	344.04	426.65	-	100	1.58
Blend / 3.6 mg Au NPs	51.68	58.52	-	391.24	-	67.51	1.07
1 MR	63.18	68.73	356.07	425.02	474.78	75.61	1.25
2 MR	62.06	67.17	-	422.64	470.02	85.13	1.48
3 MR	62.62	68.17	-	420.27	464.07	88.68	1.83
4 MR	64.86	68.17	-	421.70	461.81	72.65	1.64
5 MR	61.50	68.17	-	420.27	458.37	69.64	1.39

T_{d1}: First decomposition temperature.
T_{d1}: Second decomposition temperature.
T_d^*: New decomposition temperature.

blend/Au nanocomposite/1-5 MR in the temperature range of 301-363 K. From the Figure ure, the electrical resistivity behavior versus temperature for all studied films is described by three regions: region I (301 <T < 337 K), region II (337 <T < 351 K, region III for T > 351 K).

In region I, the electrical resistivity value increases with increasing the temperature up to 337 K. This observation is known as positive temperature coefficient (PTC) of resistivity [32] which may be mainly because of the net breakdown of conductive networks as well as the large volume expansion of the polymer with the increase in temperature up to the melting temperature. The anomalous increase in the resistivity at the melting point temperature can be assigned to the phase change of crystallites which resulted in the break- up of the conducting chains associated with increase in the resistivity [32, 33]. When the temperature is increased to the melting point of blend, a large thermal expansion of the polymer occurs due to the melting of the crystallites, producing a high PTC intensity. This phenomenon is occurred by the two factors, the number of conductive paths and the inter particle distance. The large thermal expansion of the polymer matrix can significantly increase the inter particle distance and reduce the number of conductive paths. According to the tunneling theory, the tunneling probability of an electron is related to the interparticle distance. Thus, the resistivity increases dramatically as the interparticle distance increases. The probability of electron tunneling will be very small. The PTC effect can be at least partly explained by the rapid expansion of the system undergoing melting, thereby increasing gaps between particles and aggregates and hindering the mechanism of electron tunneling [34]. Money and Swenson [28] attributed this behavior due to the existence of decoupling for the structural and conductivity relaxations in the temperature range under the melting point. The main reason for such a decoupling would likely be that sperulites grow and increase the amount of the crystalline phase in PEO/PVP blend. This crystal growth results in also rise to an "interphase" region between amorphous and crystalline regions.

In region II, at and above crystalline melting point temperature the polymeric matrix gets substantially soft with decrease in polymer viscosity. Under this condition, polymer chains are thermally agitated leading to progressive rearrangement of filler aggregates to form increased number of conductive network. Thus, conductive network formation process predominates over destruction process by thermal expansion and net resistivity decreases (NTC effect). In other words, this decrease in the resistivity is due to the re-aggregation of conductive fillers in molten polymer, generating a conductive path in the composite. According to the free volume theory, thermal movement of polymer chain segments and the dissociation of NPs will be enhanced as result from continuous increasing temperature, which that results in an increase for electrical conductivity for the prepared samples [1, 35].

In region III, the resistivity-temperature plot shows again some tendency of PTC effect at higher temperature. This PTC effect after occurrence of NTC effect at melting temperature of PEO/PVP is observed for composites which were cross-linked through curing with PEO/PVP. This existence of crosslink reduces the polymer chain motion even after melting. The crosslink network integrity is thus preserved because of chemical cross linking [32, 33].

For all studied samples, it is obvious that no linear dependence obtained in the Figure. This propose that ion conduction follows the mechanism of Williams–Landel–Ferry (WLF) not Arrhenius [1]. This observation indicates that ion transport in polymer complexes is dependent on polymer segmental motion. So, the non-linearity of the plots implies that ionic transport in the samples is associated with the polymer segmental (i.e. polymer chain) motion, which results in an increase in the free volume of the system. Thus, the segmental motion either allows the ions to hop from one site to another or provides the pathway for ions to move. In other words, the segmental motion of the polymer facilitates the translational ionic motion. For region II, there is a linear dependence of the (Ln ρ) on the reciprocal of absolute temperature. In this case, the dependence of DC conductivity (σ) can be expressed the Arrhenius equation [1]:

$$\rho = \rho exp\ (-E_a\ /KT) \tag{2}$$

where, E_a is the activation energy, K Boltzman constant and T is the absolute temperature. E_a is calculated listed in Table **1**.

It is clear that the value of electrical resistivity is largely decreased from 3.66×10^9 to 0.4×10^7 Ω.cm at 301 K after adding Au NPs. This implies that Au NPs is a good nano-filler to enhance the electrical conductivity of PEO/PVP blend. For irradiated samples, the electrical resistivity value is largely increased with
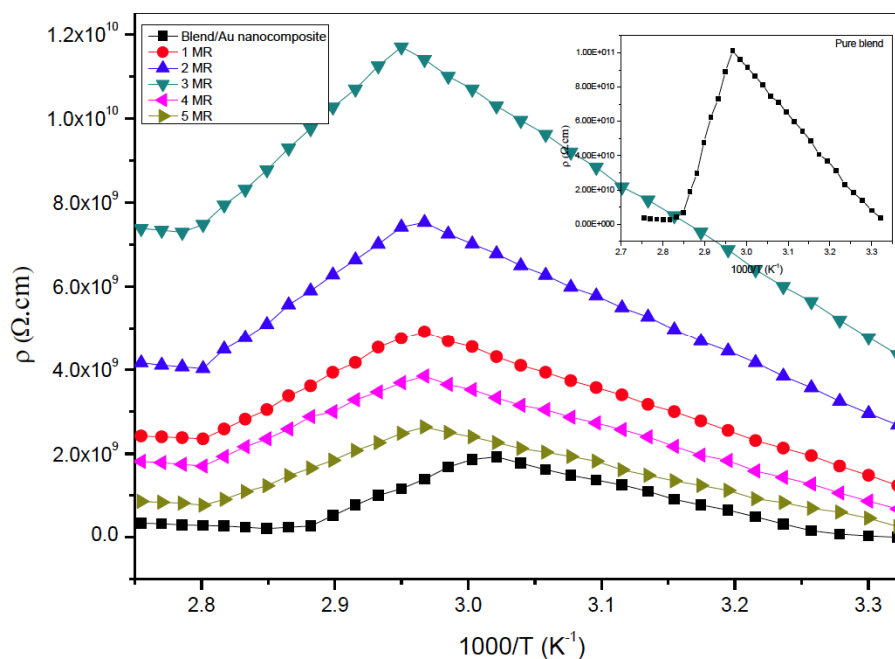
Figure 5: Variation of DC resistivity with the reciprocal of absolute temperature ($\frac{1000}{T}$ K^{-1}) for blend/Au nanocomposite and blend/Au nanocomposite/1-5 MR.
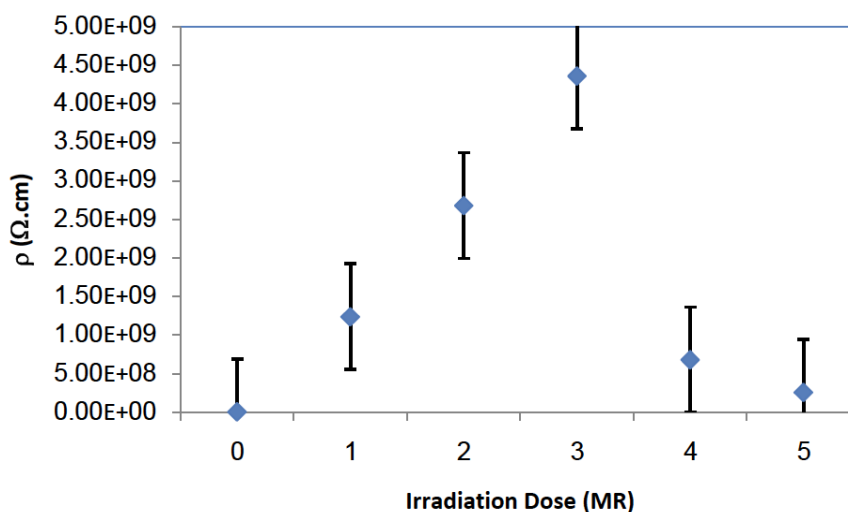
Figure 6: The variation of electrical resistivity versus irradiation dose at T=301 K for blend/Au nanocomposite (0 MR) and blend/Au nanocomposite/1-5 MR.

increasing the irradiation dose up to 3MR and is decreased for blend/Au nanocomposite/4-5 MR as shown in Figure **6**. These results are consistent with the degree of crystallinty values in DSC. The decrease of electrical resistivity value for blend/Au nanocomposite/4-5 MR can be attributed to the dispersion of Au NPs within the polymeric matrix as confirmed in SEM micrographs. Also, the PTC effect in region III for irradiated samples is partially eliminated due to γ-irradiation effects such as chain-scission reactions and cross-linking.

4. CONCLUSION

The (PEO/PVP) blend/Au nanocomposite sample was successfully prepared by casting method and exposed to different doses of γ-radiations. SEM images indicated the disappearance Au NPs aggregation on the surface for blend/Au nanocomposite/4-5 MR samples, which was occurred for blend/ Au nanocomposite. This implied that more reduction/growth for Au NPs on the polymer backbone was existed and Au NPs were dispersed within the

polymeric matrix due to high doses. The obtained results from DSC thermograms confirmed the existence of an enhancement for thermal stability through relative percentage of crystallinity calculation and the shift of T_g, T_m, T_d toward high temperatures. The electrical properties were enhanced due to Au NPs adding and varied according to the irradiation dose. Electrical characterization has revealed non-linear properties. Thus, the non-linearity of the plots suggested that ionic transport in the samples is associated with the polymer segmental motion. So, the electrical studies suggested that these films can be used in self-regulated heaters, over-current protectors and inelectrochemical devices.

REFERENCES

[1] Abdelrazek EM, Elashmawi IS, El-Khodary A, Yassin A. Structural, optical, thermal and electrical studies on PVA/PVP blends filled with lithium bromide. Curr Appl Phys 2010; 10: 607-13.
http://dx.doi.org/10.1016/j.cap.2009.08.005

[2] Abdelrazek EM, Elashmawi IS, Labeeb S. Chitosan filler effects on the experimental characterization, spectroscopic investigation and thermal studies of PVA/PVP blend films. Physica B 2010; 405: 2021-27.
http://dx.doi.org/10.1016/j.physb.2010.01.095

[3] Kumar KK, Ravi M, Pavani Y, Bhavani S, Sharma AK, Narasimha Rao VVR. Investigations on the effect of complexation of NaF salt with polymer blend (PEO/PVP) electrolytes on ionic conductivity and optical energy band gaps. Physica B 2011; 406: 1706-12.
http://dx.doi.org/10.1016/j.physb.2011.02.010

[4] Kumar KK, Ravi M, Pavani Y, Bhavani S, Sharma AK, Narasimha Rao VVR. Electrical conduction mechanism in NaCl complexed PEO/PVP polymer blend electrolytes. J Non-Cryst Solids 2012; 358: 3205-11.
http://dx.doi.org/10.1016/j.jnoncrysol.2012.08.022

[5] Abdelghany AM, Morsi MA, Abdelrazek A, Ahmed MT. Role of Silica Nanoparticles on Structural, Optical and Morphological Properties of Poly(Vinyl Chloride-co-Vinyl Acetate-co-2- Hydroxypropyl Acrylate) Copolymer. Silicon 2016; 1-6.
http://dx.doi.org/10.1007/s12633-016-9483-z

[6] Fateixa S, Daniel-da-Silva AL, Jordão N, Barros-Timmons A, Trindade T. Effect of colloidal silver and gold nanoparticles on the thermal behavior of poly (t-butyl acrylate) composites. Colloids Surf A 2013; 436: 231-36.
http://dx.doi.org/10.1016/j.colsurfa.2013.06.009

[7] Carotenuto G, Nicolais L. Synthesis and characterization of gold-based nanoscopic additives for polymers. Compos Part B Eng 2004; 35: 385-91.
http://dx.doi.org/10.1016/j.compositesb.2004.02.005

[8] Abdel-Aziz MS, Hezma A. Spectroscopic and antibacterial evaluation of nano-hydroxapatite polyvinyl alcohol biocomposite doped with microbial-synthesized nanogold for biomedical applications. Polym-Plast Technol 2013; 52: 1503-9.
http://dx.doi.org/10.1080/03602559.2013.820754

[9] Adhyapak PV, Singh N, Vijayan A, Aiyer RC, KhannaP. Single mode waveguide properties of m-NA doped Au/PVA nano-composites: Synthesis, characterization and studies. Mater Lett 2007; 61: 3456-61.
http://dx.doi.org/10.1016/j.matlet.2006.11.078

[10] Chang C-C, Chen P-H, Chang C-M. Preparation and characterization of acrylic polymer–nanogold nanocomposites from 3-mercaptopropyltrimethoxysilane encapsulated gold nanoparticles. JSol-Gel Sci Technol 2008; 47: 268-73.
http://dx.doi.org/10.1007/s10971-008-1774-4

[11] Luo J, Chu W, Sall S, Petit C. Facile synthesis of monodispersed Au nanoparticles-coated on Stöber silica. Colloids Surfac A 2013; 425: 83-91.
http://dx.doi.org/10.1016/j.colsurfa.2013.02.056

[12] Cano M, Villuendas P, Benito AM, Urriolabeitia EP, Maser WK. Carbon nanotube-supported gold nanoparticles as efficient catalyst for the selective hydrogenation of nitroaromatic derivatives to anilines. Mater Today Commun 2015; 3: 104-13.
http://dx.doi.org/10.1016/j.mtcomm.2015.02.002

[13] Hsu S-H, Chou C-W, Tseng S-M. Enhanced thermal and mechanical properties in polyurethane/Au nanocomposites. Macromol Mater Eng 2004; 289: 1096-101.
http://dx.doi.org/10.1002/mame.200400171

[14] Vodnik VV, Abazović ND, Stojanović Z, Marinović-Cincović M, Mitrić M, Čomor MI. Optical, structural and thermal characterization of gold nanoparticles–poly (vinylalcohol) composite films. J Compos Mater 2012; 46: 987995.
http://dx.doi.org/10.1177/0021998311413624

[15] Abdelrazek EM, El Damrawi G, Elashmawi IS, El-Shahawy A. The influence of γ-irradiation on some physical properties of chlorophyll/PMMA films. Appl Surf Sci 2010; 256: 2711-18.
http://dx.doi.org/10.1016/j.apsusc.2009.11.015

[16] Eisa WH, Abdel-Moneam YK, Shaaban Y, Abdel-Fattah AA, Zeid AMA. Gamma-irradiation assisted seeded growth of Ag nanoparticles within PVA matrix. Mater Chem Phys 2011; 128: 109-13.
http://dx.doi.org/10.1016/j.matchemphys.2011.02.076

[17] Abdelghany AM, Abdelrazek EM, Badr SI, Morsi MA. Effect of gamma-irradiation on (PEO/PVP)/Au nanocomposite: Materials for electrochemical and optical applications. Mater Des 2016; 97: 532-43.
http://dx.doi.org/10.1016/j.matdes.2016.02.082

[18] Abdelghany AM, Abdelrazek EM, Badr SI, Abdel-Aziz MS, Morsi MA. Effect of Gamma-irradiation on biosynthesized gold nanoparticles using *Chenopodium murale* leaf extract. J Saudi Chem Soc 2015.
http://dx.doi.org/10.1016/j.jscs.2015.10.002

[19] Kulasekarapandian K, Jayanthi S, Muthukumari A, Arulsankar A, Sundaresan B. Preparation and characterization of PVC–PEO based polymer blend electrolytes complexed with Lithium perchlorate. Int J Eng Res Dev 2013; 5: 30-39.

[20] Saroj AL, Singh RK, Chandra S. Thermal, vibrational, and dielectric studies on PVP/LiBF$_4$+ ionic liquid [EMIM][BF$_4$]-based polymer electrolyte films. J Phys Chem Solids 2014; 75: 849-57.
http://dx.doi.org/10.1016/j.jpcs.2014.02.005

[21] Baykal A, Bıtrak N, Ünal B, Kavas H, Durmus Z, Özden Ş, *et al.* Polyol synthesis of (polyvinylpyrrolidone) PVP–Mn$_3$O$_4$ nanocomposite. J Alloys Compds 2010; 502: 199-205.
http://dx.doi.org/10.1016/j.jallcom.2010.04.143

[22] Sivaiah K, Kumar KN, Naresh V, Buddhudu S. Structural and optical properties of Li$^+$: PVP & Ag$^+$: PVP polymer films. Mater Sci Appl 2011; 2: 1688-96.
http://dx.doi.org/10.4236/msa.2011.211225

[23] Liu Y, Lee JY, Hong L. Morphology, crystallinity, and electrochemical properties of in situ formed poly (ethylene oxide)/TiO$_2$ nanocomposite polymer electrolytes. J Appl Polym Sci 2003; 89: 2815-22.

[24] Lee J, Bhattacharyya D, Easteal AJ, Metson JB. Properties of nano-ZnO/poly (vinyl alcohol)/poly (ethylene oxide) composite thin films. Curr Appl Phys 2008; 8: 42-47.
http://dx.doi.org/10.1016/j.cap.2007.04.010

[25] Johan MR, Shy OH, Ibrahim S, Yassin SMM, Hui TY. Effects of Al_2O_3 nanofiller and EC plasticizer on the ionic conductivity enhancement of solid PEO–$LiCF_3SO_3$ solid polymer electrolyte. Solid State Ion 2011; 196: 41-47.
http://dx.doi.org/10.1016/j.ssi.2011.06.001

[26] Karmakar A, Ghosh A. Poly ethylene oxide (PEO)–LiI polymer electrolytes embedded with CdO nanoparticles. J Nanopart Res 2011; 13: 2989-96.
http://dx.doi.org/10.1007/s11051-010-0194-x

[27] Kumar KK, Ravi M, Pavani Y, Bhavani S, Sharma AK, Narasimha Rao VVR. Investigations on PEO/PVP/NaBr complexed polymer blend electrolytes for electrochemical cell applications. J Membr Sci 2014; 454: 200-11.
http://dx.doi.org/10.1016/j.memsci.2013.12.022

[28] Money BK, Swenson J. Dynamics of poly (ethylene oxide) around its melting temperature. Macromolecules 2013; 46: 6949-54.
http://dx.doi.org/10.1021/ma4003598

[29] Przyłuski J, Such K, Wyciślik H, Wieczorek W, Floriańczyk Z. PEO-based polymer blends as materials for solid electrolytes. Synth Met 1990; 35: 241-47.
http://dx.doi.org/10.1016/0379-6779(90)90048-P

[30] Peng Z, Kong LX. A thermal degradation mechanism of polyvinyl alcohol/silica nanocomposites. Polym Degrad Stab 2007; 92: 1061-71.
http://dx.doi.org/10.1016/j.polymdegradstab.2007.02.012

[31] Mansour SA. Study of thermal stabilization for polystyrene/carbon nanocomposites via TG/DSC techniques. J Therm Anal Calorim 2013; 112: 579-83.
http://dx.doi.org/10.1007/s10973-012-2595-9

[32] Rahaman M, Chaki TK, Khastgir D. Control of the temperature coefficient of the DC resistivity in polymer-based composites. J Mater Sci 2013; 48: 7466-75.
http://dx.doi.org/10.1007/s10853-013-7561-9

[33] Zhang C, Ma C-A, Wang P, Sumita M. Temperature dependence of electrical resistivity for carbon black filled ultra-high molecular weight polyethylene composites prepared by hot compaction. Carbon 2005; 43: 2544-53.
http://dx.doi.org/10.1016/j.carbon.2005.05.006

[34] Yoon K-B, Lee GH, Choi WY, Lee D-H. Electrical properties of non-crosslinked polyethylene/syndiotactic polystyrene composites filled with carbon black. Polym J 2007; 39: 1143-49.
http://dx.doi.org/10.1295/polymj.PJ2007046

[35] Bhargav PB, Sarada BA, Sharma AK, Narasimha Rao VVR. Electrical conduction and dielectric relaxation phenomena of PVA based polymer electrolyte films. J Macromol Sci Part A: Pure Appl Chem 2009; 47: 131-37.
http://dx.doi.org/10.1080/10601320903458564